INSTITUTE OF PHYSICS PUBLISHING JOURNAL OF PHYSICS: CONDENSED MATTER

J. Phys.: Condens. Matter **15** (2003) 3069–3078 PII: S0953-8984(03)58408-9

Tetragonal and rhombohedral induced polar order from the relaxor state of $PbZn_{1/3}Nb_{2/3}O_3$

A Lebon[1,2]**, H Dammak and G Calvarin**

Structures, Propriétés et Modélisation des Solides, UMR 8580, CNRS—Ecole Centrale Paris, Grande Voie des Vignes, 92295 Châtenay-Malabry Cedex, France

E-mail: a.lebon@fkf.mpg.de

Received 16 January 2003
Published 6 May 2003
Online at stacks.iop.org/JPhysCM/15/3069

Abstract

Structural and dielectric characterizations of the relaxor ferroelectric $PbZn_{1/3}Nb_{2/3}O_3$ (PZN) were carried out on single crystals in the temperature range of the dielectric anomaly (370 K $< T <$ 440 K), under dc electric field applied along [001]- and [111]-directions. Two ferroelectric phases, tetragonal (T) and rhombohedral (R), can be field induced in this temperature range, the symmetry of which depends on the direction of the applied field, [001] and [111] respectively. E–T diagrams were built and interpreted under the consideration of polar nano-regions (PNRs) with a prominent tetragonal component. These PNRs prevent the onset of a monodomain state when the field is applied along [111] and explain the features of PZN for an applied field along [001]: large lattice strain, easy onset of the T phase and suppression of the dielectric relaxation for $E \geqslant 1.5\,\mathrm{kV\,cm^{-1}}$. The microscopic origin of these PNRs can be discussed in relation with recent nuclear magnetic resonance and structural results reported in other isomorphous relaxors.

1. Introduction

Relaxor ferroelectrics are characterized by a broad dielectric maximum that depends on both frequency and temperature, and a large dielectric dispersion. Over the years, the relaxor behaviour has been described in terms of the formation, in the cubic paraelectric matrix, of polar nano-regions (PNRs) [1]. Recent ^{207}Pb and ^{93}Nb nuclear magnetic resonance (NMR) results on $PbMg_{1/3}Nb_{2/3}O_3$ (PMN), the textbook relaxor, have brought new evidence of the existence of PNRs. On the NMR timescale, the polar clusters are dynamic entities with variable orientation and magnitude of the local polarization [2]; on the other hand, the existence of

[1] Current address: Festkörperforschung, Max Planck Institut, 1, Heisenbergstrasse, 70569 Stuttgart, Germany.
[2] Author to whom any correspondence should be addressed.

Mg:Nb disordered microregions with ⟨001⟩ (65%), ⟨011⟩ (15%) and ⟨111⟩ (15%) directions of niobium ion shifts was shown [3].

$PbZn_{1/3}Nb_{2/3}O_3$ (PZN) is another relaxor ferroelectric ($T_{max} = 405$ K for $\omega = 100$ Hz). The existence of PNRs was also assumed in this compound to explain the occurrence, below $T = 440$ K, of diffuse scattering centred on the Bragg reflections [4]. The correlation length (ξ) of this diffuse scattering at $T_{max,\omega=100\ Hz}$ is equal to 10 nm and continues to grow at lower temperature: $\xi = 15$–18 nm at $T = 300$ K [4]. This scattering was assigned to the existence of PNRs in PZN. Moreover, in contrast with PMN, PZN exhibits a spontaneous phase transition towards a rhombohedral ferroelectric phase [5]. A recent high-resolution x-ray diffraction study on single crystals has shown that the cubic (C) $\rightarrow$ rhombohedral (R) phase transition spreads over the temperature range $T_{CR} = 385(5)$ K–$T_R = 325(5)$ K [6]. Below T_{CR}, the C-phase transforms progressively into R-domains of average size 60–70 nm along the [111]-directions that do not grow as temperature is lowered. At T_R, the R-microdomains fully pave the crystal but residual regions could exist between the R-domains. Taking these results for granted, the low-temperature phase is a coexistence between R-domains of 60–70 nm size and PNRs of 15–20 nm size. The question of the nature of the PNRs naturally arises, and of course it seems more adequate to study them in the region of T_{max} without being disturbed by the R-domain states.

The present paper is a study of the structural and dielectric behaviours of PZN under electric field, in the temperature range of the relaxor cubic (C) phase, as a function of the applied field directions [111] and [001]. The comparison between these two directions of polarization was prompted by the larger fraction of the niobium atom that shifts along [001] than along [111]. Electric field–temperature (E–T) diagrams were built using high-resolution x-ray diffraction, dielectric and pyroelectric measurements on oriented single crystals. This method is nicely adapted to probe the anisotropy of the so-called PNRs.

2. Experimental details

PZN single crystals were grown in a platinum crucible by a flux method, with lead oxide excess [7, 8]. They were extracted from the flux with the aid of a warm 25 vol% nitric acid solution. Yellow transparent crystals were oriented and cut using the Laue technique. Two crystals of the same batch cut along (100) and (111) of a platelet shape ($3 \times 2 \times 0.5$ mm^3) were devoted to the electric characterization: pyroelectric current and dielectric susceptibility. A third crystal of rhombus shape, cut along the directions [001], [100] and [110], was used for the x-ray diffraction experiments with the electric field applied along [001]. The [111] oriented crystal was previously studied by diffraction [6]. Before the gold electrode sputtering, all crystals were polished and annealed at 450 °C to remove residual stresses.

Dielectric and pyroelectric current measurements were performed with an HP4192A impedance analyser (Hewlett Packard) and collected under zero-field cooling (ZFC) and field cooling (FC) processes. For dielectric data, a dc electric field was added to the oscillating signal of weak amplitude. Pyroelectric current was measured during FC runs (1 K min^{-1}) and also during increasing field runs (0.2 kV cm^{-1} min^{-1}) at a given temperature.

The x-ray diffraction diagrams were recorded in Bragg–Brentano geometry with a high-accuracy two-axis diffractometer built up in the laboratory [9]. Experimental details and sample mounting have been reported elsewhere [6]. To build the E–T diagrams, the field was first increased at a certain value with constant steps and maintained for 5 min before recording and then further increased. This process was repeated for all the possible geometries.

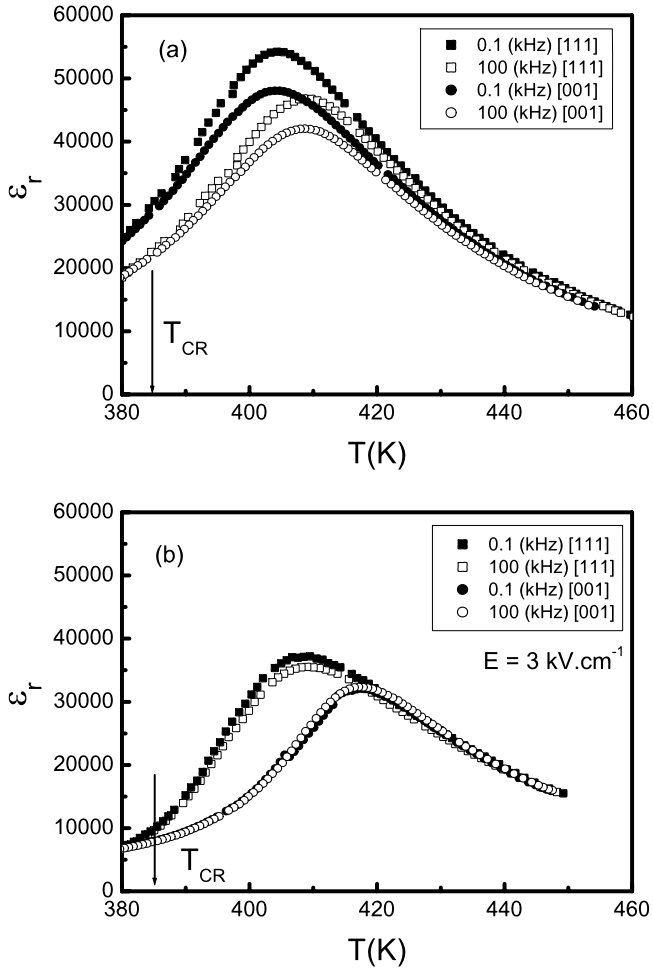

Figure 1. Real part of the dielectric permittivity, at $\omega = 0.1$ and 100 kHz, of crystals [111] (■ and □) and [001]) (● and ○): (a) in the ZFC regime; (b) in the FC regime with $E = 3$ kV cm^{-1}.

3. Results

3.1. Dielectric characterization

Figure 1 shows the temperature dependence of the real part of the dielectric permittivity (ε_r) of [001] and [111] single crystals, for two frequencies $\omega = 0.1$ and 100 kHz. In the ZFC run (figure 1(a)), the dielectric permittivity of both oriented crystals exhibits a strong frequency dependence of ε_{max} and T_{max} that is characteristic of relaxor ferroelectrics. On the other hand, in the FC run (figure 1(b)), the dielectric dispersion is suppressed for [001] and strongly attenuated for [111], which is rather reminiscent of classical ferroelectrics. However, a noteworthy difference between the two directions is observed: the increase of T_{max}, with respect to the ZFC run, is stronger for the [001] direction, 14 K against 6 K for the [111]-direction.

Table 1. Cell parameters and lattice strains, at $T = 400$ K, for the two induced ferroelectric phases: tetragonal ($E \parallel [001]$) and rhombohedral ($E \parallel [111]$).

$E \parallel [001]$	a (Å)	c (Å)	V (Å^3)	$(c(E) - a(E))/a(0)$
Cubic	4.0615(4)		66.99(1)	0
Tetragonal	4.0574(4)	4.0694(4)	66.99(1)	28.1×10^{-3}
$E \parallel [111]$	a (Å)	α (deg)	V (Å^3)	$\Delta\alpha/\alpha$
Cubic	4.0616(5)	90	67.00(1)	0
Rhombohedral	4.0607(5)	89.98	66.96(1)	2×10^{-4}

3.2. Structural characterization

Figure 2 displays the (004), (400), (330) and (333) diffraction peaks recorded at 400 K, first without electric field, then under a 4 kV cm^{-1} field applied along [001] and finally after removal of the field ($E = 0$ after 4 kV cm^{-1}). Under applied electric field, the (004) peak is shifted towards low 2θ-angles while the (400), (330) and (333) peaks are shifted towards high 2θ-angles. These angular shifts are related, respectively, to an increase of the reticular distance $d_{(004)}$ ($\Delta d/d = +19.3 \times 10^{-3}$) and to a decrease of $d_{(400)}$ ($\Delta d/d = -9.8 \times 10^{-3}$), $d_{(330)}$ ($\Delta d/d = -9.8 \times 10^{-3}$) and $d_{(333)}$ ($\Delta d/d = -2.7 \times 10^{-4}$). The relative decrease $\Delta d/d$ is equal for the (400) and (330) peaks, within experimental error. These changes of the cubic cell are consistent with a tetragonal distortion[3]; the tetragonal (T) cell parameters are given in table 1. The diffraction peaks recover their initial angular position after removal of the electric field; so, the induced C $\rightarrow$ T symmetry change is reversible.

Figure 3 shows the (333) and (005) diffraction peaks recorded at $T = 400$ K, under zero and 4 kV cm^{-1} field applied along [111]. The (333) peak is shifted towards the low-2θ side (figure 3(a)), while (005) is very slightly shifted towards the high-2θ side. These shifts are consistent with a rhombohedral distortion; the cell parameters are given in table 1. As for [001], the induced C $\rightarrow$ R symmetry change is reversible.

Figure 4 displays the dependence on electric field, at $T = 400$ K, of the longitudinal strain $S_{33} = \Delta d/d$, along the directions [001] and [111] of the applied field. The $S_{33} = f(E)$ curves exhibit an inversion of curvature for both directions. S_{33} is lower along [111] and the difference increases with E.

The dependence on E of the tetragonal strain $e_S = (c(E) - a(E))/a(0) = S_{33} - S_{31}$ is shown in figure 5, for different temperatures; S_{33} (longitudinal strain) $= c(E)/a(0)$ and S_{31} (transverse strain) $= a(E)/a(0)$. For any E, the lower the temperature the higher e_S, S_{33} and S_{31}. All the $e_S(E)$ and $S_{ij}(E)$ (not plotted here) curves exhibit an inversion of curvature for, respectively, $e_S \approx 0.08$, $S_{33} \approx 0.05$ and $S_{31} \approx -0.03$ (in%). These strain values do not depend on temperature, within the limit of the measurement precision. This tetragonal strain dependence, as a function of electric field, is characteristic of a phase transition between an electrostrictive C phase and a field-induced piezoelectric T phase.

3.3. Electric field–temperature diagram

Pyroelectric current measurements were performed in order to investigate the onset of polarization associated with the structural changes. Figure 6 shows the temperature dependence of the pyroelectric current I and of the integrated polarization P, for different values of applied field along [001]. For $E > 0.33$ kV cm^{-1}, the higher E the higher the temperature

[3] The volume change $\Delta V/V$, which is equal to $\Delta c/c + 2\Delta a/a$, is about -3×10^{-4}.

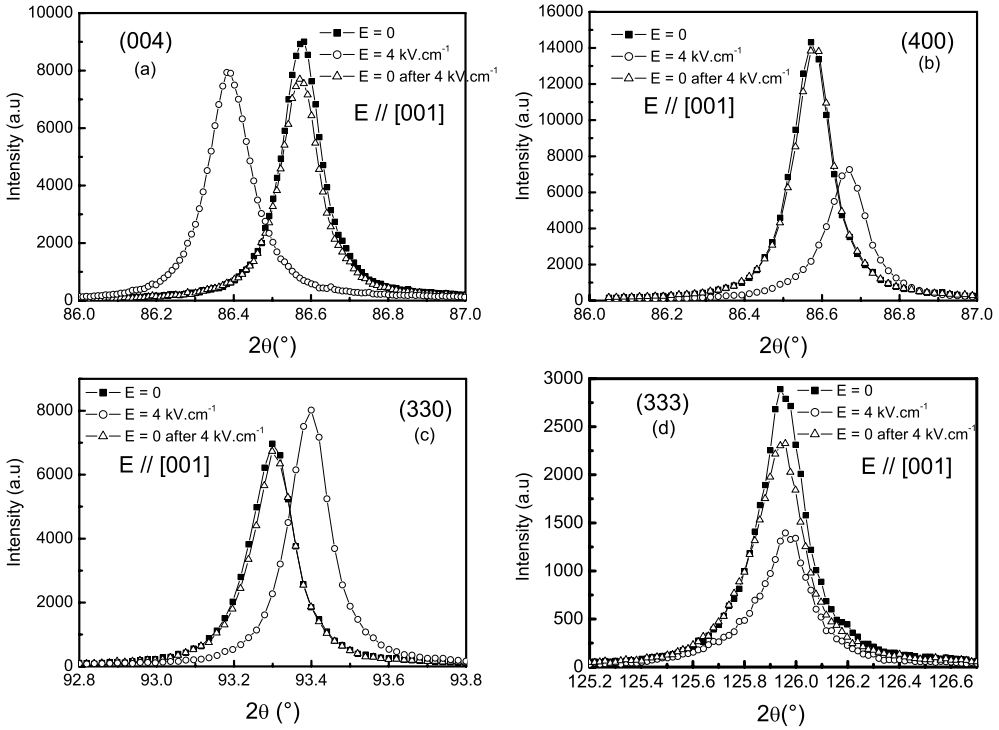

Figure 2. Diffraction peaks: (a) (004), (b) (400), (c) (330) and (d) (333), recorded at $T = 400$ K on the [001] crystal, with $E = 0$ (■), $E = 4$ kV cm^{-1} (○) and $E = 0$ after 4 kV cm^{-1} (△).

of pyroelectric current peak (I_{max}) and the broader the polarization peak as a function of temperature. All the $P(E)$ curves exhibit an inversion of curvature for a value of polarization ($P \approx 0.13$ C m^{-2}) which does not depend on electric field, within the measurement precision. Below about $T_{CR} = 385 \pm 5$ K, the temperature dependence of polarization is similar whatever the electric field is. For $E \leqslant 0.33$ kV cm^{-1}, the polarization is only partial ($P = 0.07$ C m^{-2}, at 380 K, for $E = 0.33$ kV cm^{-1}). These temperature and electric field dependences of polarization are characteristic of a field-induced C (paraelectric) $\rightarrow$ ferroelectric phase transition.

An E–T diagram was built from structural and polarization results (figure 7(a)). The couple of values (E, T), plotted on this diagram, stands for the inflexion point of $e_S = f(E)$ and $P = f(T)$ curves, figures 5 and 6 respectively. The values of T_{max} of dielectric permittivity, measured for different values of E, are also plotted for comparison. A striking agreement is observed between the structural and polarization data, which lie on a common line. So, this line corresponds to a transition between a paraelectric (electrostrictive) C phase and a field-induced ferroelectric (piezoelectric) T phase. The lower E the lower the temperature of the phase transition; in the temperature range around $T_{CR} = 385 \pm 5$ K, the threshold field to induce the T phase is $E \approx 0.4(1)$ kV cm^{-1}. No frequency dispersion of dielectric permittivity is observed for $E \geqslant 1.5$ kV cm^{-1}; in this electric field range, T_{max} becomes equal to the temperature of the C $\rightarrow$ T phase transition. Below $E = 1.5$ kV cm^{-1}, T_{max} is frequency dependent; so, its physical meaning is related to the size distribution of the PNRs [1].

A similar E–T diagram was built for the [111]-direction of the applied field (figure 7(b)), from present diffraction data and previously reported polarization results [10]. In contrast to

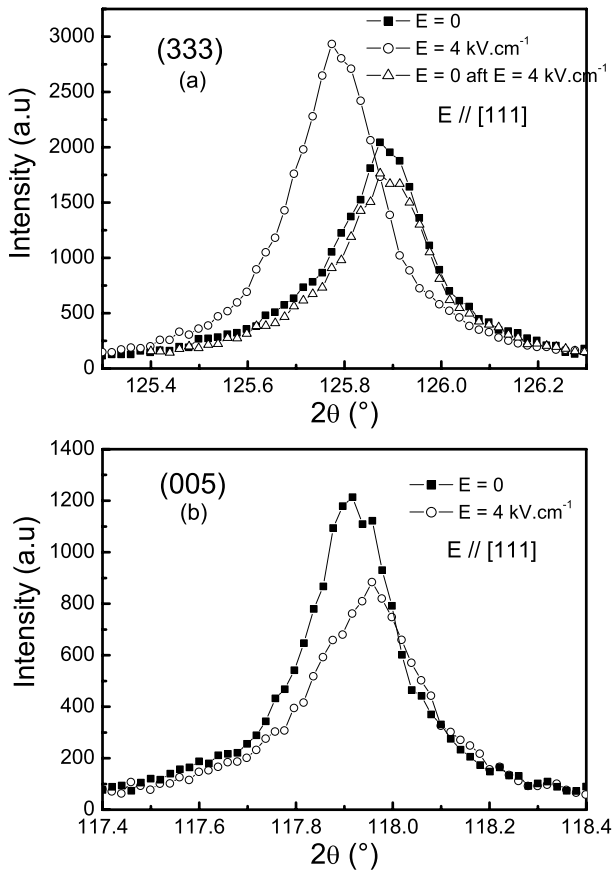

Figure 3. Diffraction peaks: (a) (333); (b) (005); recorded at $T = 400$ K on the [111] crystal, with $E = 0$ (■), $E = 4$ kV cm^{-1}(○) and $E = 0$ after 4 kV cm^{-1} (△).

the [001] diagram, the lattice strain and polarization lines are separate. In the E–T region below the lattice strain line the phase is cubic and electrostrictive, while in the region above the 'polarization' line the induced ferroelectric phase is rhombohedral. The phase diagram exhibits an intermediate phase whose structural features will be discussed in the following section.

For $E \geqslant 3$ kV cm^{-1}, the values of $T_{\max}$ are located close to the polarization line and no frequency dispersion is observed on the dielectric permittivity; so, $T_{\max}$ is closely related to the transition into the R phase. Below $E = 3$ kV cm^{-1}, $T_{\max}$ is frequency dependent and its behaviour is characteristic of a relaxor ferroelectric.

3.4. Discussion

Combined x-ray diffraction and pyroelectric current experiments, performed on [001] and [111] oriented PZN single crystals, as a function of temperature and electric field, revealed that two different ferroelectric phases could be field induced in the temperature range of the relaxor cubic phase. The symmetry of the ferroelectric phase, T or R, depends on the direction of applied field, [001] or [111] respectively. Above T_{CR}, the field required to induce the ferroelectric phase is lower for the T symmetry than that for the R one; at $T = 400$ K,

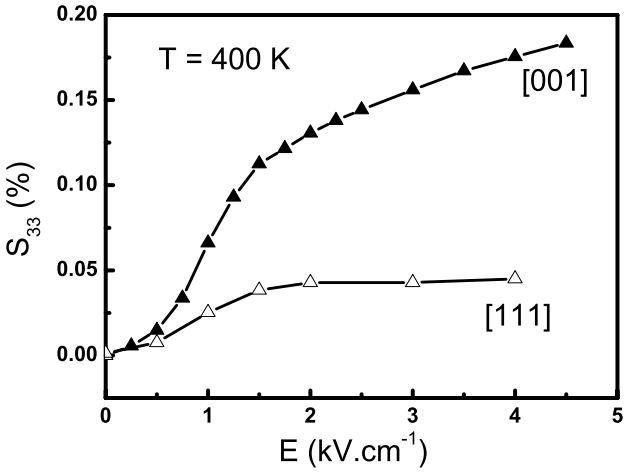

Figure 4. Induced longitudinal strain $S_{33} = \Delta d/d$, at $T = 400$ K, for the two [001] and [111] crystals, as a function of applied electric field E. Continuous curves are guides for the eyes.

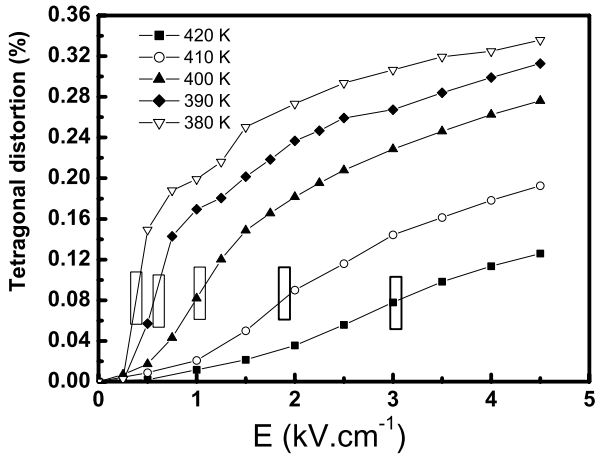

Figure 5. Electric field dependence of the tetragonal strain $e_S = (c(E) - a(E))/a(0)$ of the [001]-oriented crystal, at $T = 380$, 390, 400, 410 and 420 K (the rectangles symbolize the inflexion points of the $e_S(E)$ curves). Continuous curves are guides for the eyes.

$E = 1.0$ and 2.6 kV cm^{-1}, respectively (figures 7(a) and (b)). Around T_{CR}, this field is very close, $E \approx 0.5$ kV cm^{-1}. Below T_{CR}, the induced T phase becomes less stable than the R one; indeed, a C–R phase transition takes place from T_{CR}, even without applying field [6], while the T phase can be observed only down to $T = 370$ K (with $E \geqslant 0.4$ kV cm^{-1}), the temperature from which a tetragonal $\rightarrow$ monoclinic phase transition takes place [11]. These results indicate that the structural behaviour of PZN, in the temperature range of the dielectric anomaly, is characterized by the existence of two different long-range polar orders having very close free energy. This agrees with the idea recently developed in theoretical papers that states that the free energy becomes flat and isotropic in the morphotropic phase boundary where several phases with different symmetry, i.e. R, M_A, O, M_C and T, could be stabilized [12]. The electric field plays the role of titanium, in other words the morphotropic phase boundary could

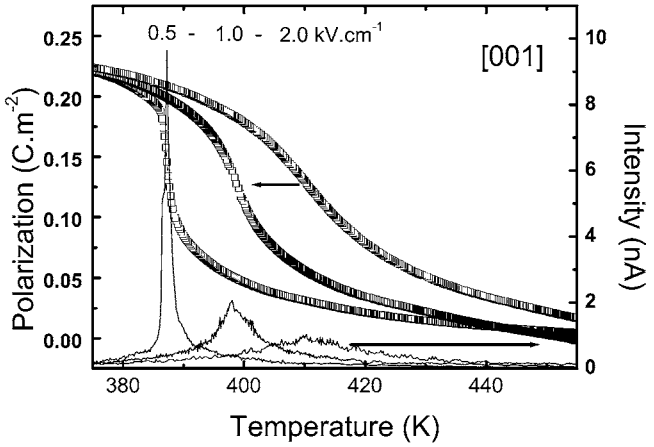

Figure 6. Pyroelectric current and derived polarization of the [001]-oriented crystal, measured during an FC run, for $E = 0.5$, 1.0 and 2.0 kV cm^{-1}.

be approached under electric field and a tetragonal or rhombohedral phase could actually be observed. This idea was also checked in the solid solution of PZN with lead titanate [13].

When the field is applied along [001], the C (electrostrictive) $\rightarrow$ T (ferroelectric) induced phase transition is direct; on the other hand, when E is applied along [111], the C phase first transforms into an intermediate phase, characterized by the absence of a long-range polar order, before transforming into a ferroelectric R phase. By noticing that

(i) the lattice strain line crosses the temperature axis of the E–T diagram close to T_{CR} (figure 7(b)), within the limit of the experimental error, and
(ii) without field ($E = 0$), the C phase transforms progressively into nanometric R-domains ($\approx$70 nm) below T_{CR} [6],

it could be thought that the intermediate region of the [111] diagram consists in progressive nucleation of nanometric R-domains into the C phase (so-called microdomain state). This interpretation is quite consistent with the optical observations of Mulvihill *et al* [14]; indeed, birefringence related to the induction of polar 'microdomains' was evidenced in the E–T intermediate region. The polarization line corresponds to the transition R microdomain $\rightarrow$ R macrodomain. During this transition the so-called microdomains (20–100 nm in size) transform into macrodomains (some micrometres in size) with creation of well defined domain walls. Mulvihill *et al* [14] did observe such a transition line from birefringence measurements, but this line was reported to be nearly vertical at T_{CR}. In fact, optical measurements were performed regardless of kinetic effects, but we have shown that at low field these effects affect the transition lines of E–T diagrams [10].

For any couple of E–T values, the longitudinal strain S_{33} is higher according to the [001]-direction of the field. This strongly suggests that the dipole moment within PNRs aligns preferentially along this direction. On the other hand, even when a strong electric field of 15 kV cm^{-1} is applied along [111], one cannot obtain an R monodomain state [14], that strongly suggests the existence of non-rhombohedral regions between the R macrodomain. As a conclusion, it can be derived that PNRs have a prominent T component. This preferential polar order of the relaxor state has some microscopic origin that has to be found in the literature for some other relaxor since reports on PZN are rather few. The first microscopic evidence comes from a structural study, at $T = 300$ K, of the isomorphous $Pb(Mg_{1/3}Nb_{2/3})_{0.9}Ti_{0.1}O_3$

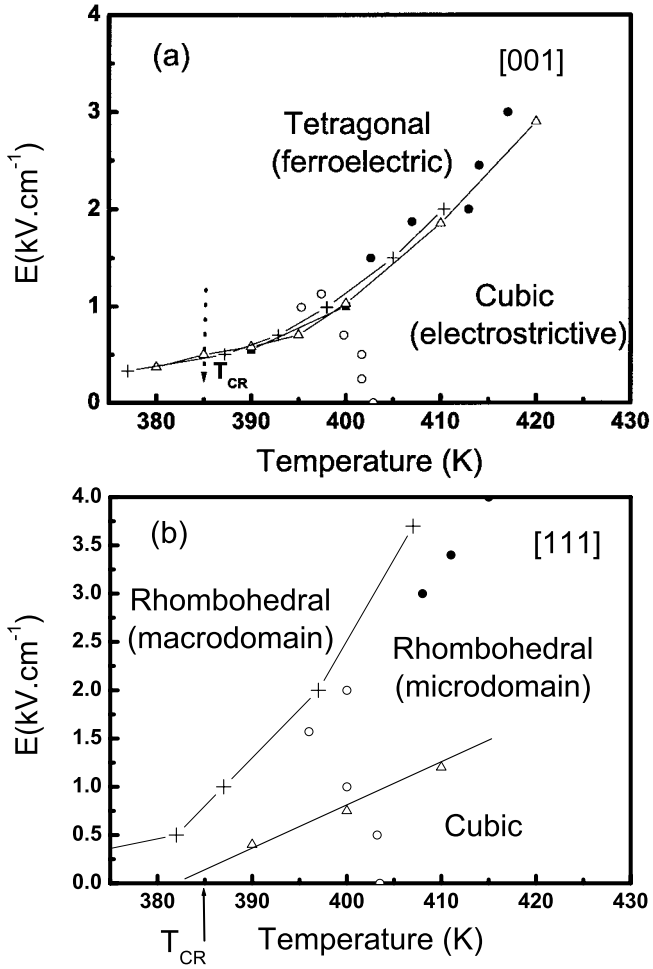

Figure 7. E–T diagrams for the poled crystals along the directions (a) [001] and (b) [111]. △ and + stand for the inflexion points of $e_S = f(E)$ and $P = f(T)$ curves, respectively. The two points ■, plotted at $T = 390$ and 400 K in (a), correspond to polarization data determined by poling the crystal at a constant temperature with an increasing field from 0 to 4 kV cm^{-1}. (●) and (○) stand respectively for T_{max} when it is frequency independent and when it is frequency dependent (values plotted for $\omega = 100$ Hz), as a function of E. Continuous curves are guides for the eyes.

(PMN-PT 10%) [15] that undergoes a spontaneous C → R phase transition ($T_{CR} = 285$ K). It is found that the lead atom is disordered along the six ⟨001⟩ directions with $\delta = 0.22$ Å and, more importantly, that the observed diffuse scattering is associated with a start of the divergence at $T = 400$ K in the lead disorder. The second strong result is an NMR study performed on ^{93}Nb on the isomorphous PMN [3]. The authors analyse the ^{93}Nb NMR line shape obtained at $T = 450$ K, i.e. in the C paraelectric phase, and show that, in the Mg/Nb chemically disordered regions of the matrix, the niobium ions shift prominently along the ⟨001⟩ direction (65%) instead of the ⟨110⟩ and ⟨111⟩ directions (both 15%). If we assume that these microscopic features are common to other relaxors like PZN, it sheds some light on our results and enables us to consider PZN as a very inhomogeneous material with competing T and R polar order. When the field is applied along [111] the ratio of the Nb ions that shift along [111] increases

and, meanwhile, the lead ion reduces its disorder from six ⟨001⟩ positions to three with respect to the [111]-direction of the field. In contrast, when the field is applied along [001], the lead disorder is suppressed and the ratio of niobium oriented along [001] increases. Only when a critical field overcomes the thermal agitation does the whole C matrix transform into a T ferroelectric phase. Our results indicate that the transformation takes place when critical values of lattice strain ($e_S = 0.08\%$) and of polarization ($P = 0.13$ C m^{-2}) are reached.

4. Conclusion

In summary, the coupled structural and electrical study evidenced the possibility of inducing R and T ferroelectric phases for electric field applied along [111] and [001], respectively. The two induced phases must have very close free energy. The comparison of the two E–T diagrams, the dielectric behaviour and the respective lattice strain values indicates that the [001]-direction is by far the most 'favourable' for inducing a ferroelectric phase in the temperature range of the dielectric anomaly. A possible microscopic explanation is the existence of PNRs with a prominent T polarization; most of our results can be interpreted within the model of relaxors developed by Blinc *et al* [2]. The change of the preferential direction of the Nb ion shift under electric field and the lead disorder along ⟨001⟩-directions provide a qualitative microscopic argument for the selection of the direction of polarization by the direction of the electric field. This report is evidence that the effect of the direction of polarization should be investigated more keenly in the temperature range of the dielectric anomaly, for instance in some other compounds such as the textbook relaxor PMN.

References

[1] Cross L E 1987 *Ferroelectrics* **76** 241
[2] Blinc R, Gregorovic A, Zalar B, Pirc R, Laguta V V and Glinchuk M D 2001 *Phys. Rev.* B **63** 024104
[3] Glinchuk M D, Nokhrin S N, Bykov I B, Laguta V V, Blinc R, Gregorovic A and Zalar B 2001 *Phys. Status Solidi* **228** 757
[4] La-Orauttapong D, Toulouse J, Robertson J L and Ye Z G 2001 *Phys. Rev.* B **64** 212101
[5] Yokomizo Y, Takahashi T and Nomura S 1970 *J. Phys. Soc. Japan* **28** 1278
[6] Lebon A, Dammak H and Calvarin G 2002 *J. Phys.: Condens. Matter* **14** 7035
[7] Mulvihill M L, Park S E, Risch G, Li Z and Uchino K 1996 *Japan. J. Appl. Phys.* **35** 3984
[8] Ould I A 1997 *PhD Thesis* Ecole Centrale de Paris (in French)
[9] Berar J F, Calvarin G and Weigel D 1980 *J. Appl. Crystallogr.* **13** 201
[10] Dammak H, Lebon A and Calvarin G 1999 *Ferroelectrics* **235** 151
[11] Lebon A, Dammak H and Calvarin G 2003 to be submitted
[12] Ishibashi Y and Iwata M 1999 *Japan. J. Appl. Phys.* **38** 1454
[13] Lu Yu, Jeong D-Y, Cheng Z-Y, Shrout T and Zhang Q M 2002 *Appl. Phys. Lett.* **80** 1918
[14] Mulvihill M L, Cross L E, Cao W and Uchino K 1997 *J. Am. Ceram. Soc.* **80** 1462
[15] Dkhil B, Kiat J M, Calvarin G, Baldinozzi G, Vakhrushev S B and Suard E 2002 *Phys. Rev.* B **65** 1061